

INJECTION LOCKING OF AN IMPATT DIODE OSCILLATOR BY USING A LOW-FREQUENCY SIGNAL
PARAMETRIC INJECTION LOCKING

Hiroshi OKAMOTO and Mutsuo IKEDA
Musashino Electrical Communication Laboratory
Nippon Telegraph and Telephone Public Corporation
Musashino-shi, Tokyo 180, JAPAN.

Abstract

A new injection locking process is proposed and demonstrated experimentally, where a low-frequency injection signal can be used to lock an ultra-high frequency solid-state oscillator. This process has much wider locking bandwidth than the conventional subharmonic injection locking.

Introduction

Injection locking is a circuit technology useful to reduce sideband noise of solid-state ultra-high frequency oscillators. Three kinds of injection locking processes are known. They are;

- (1) The fundamental-wave injection locking¹, in which $f_{inj} \approx f_0$ where f_{inj} and f_0 are frequencies of the injection signal and the free-running oscillation to be locked, respectively. This is the most conventional process.
- (2) The subharmonic injection locking², in which $f_{inj} \approx (1/n)f_0$ where $n=2,3,4$
- (3) The sideband-wave injection locking³, in which two injection signals are used, one of which is of low-frequency $f_{inj,1}$ and the other of the frequency $f_{inj,2} \approx f_0 + f_{inj,1}$.

The processes of (1) and (2) have much wider locking bandwidth (more than 100 MHz) at a certain injection power than the second one, but it is necessary to realize a low noise injection signal source whose frequency is as high as that of the oscillator to be stabilized. In the second process, on the other hand, a low-frequency signal source can be used in injection, but unfortunately, the locking bandwidth becomes narrower when increasing the order of multiplication n . Take the subharmonic injection locking of 8.5 GHz IMPATT oscillator, for instance. Not more than 1 MHz of the locking bandwidth is reported² to be available when $n=9$ and the locking gain of 0 dB.

In this report, a new injection locking process, called parametric injection locking, is proposed, which has following two features;

- (1) The frequency of the injection signal can be much lower than that of the solid-state oscillator to be stabilized, and can be selected arbitrarily.
- (2) Wide locking bandwidth can be obtained, which is comparable with that in the first and the third processes described above.

Experimental demonstration by using a millimeter-wave IMPATT diode oscillator will be given here, along with some analytical explanation.

Mechanism

In the vicinity of the main resonator which determines the free-running oscillation frequency f_0 of an IMPATT diode, another high-Q cavity resonator which is called an idler resonator is provided, whose resonant frequency f_i is set at a few GHz apart from f_0 . When a signal with frequency f_{inj} which is nearly equal to the difference frequency $|f_0 - f_i|$ is injected, many sideband-waves are produced, whose frequencies are $f_u = f_0 + f_{inj}$, $f_L = f_0 - f_{inj}$ and so on.

Then, one of these frequencies, f_u or f_L , which lies nearer to f_i is trapped by the idler cavity and kept invariant when changing f_{inj} . As a consequence, the oscillation-wave frequency begins to change linearly

in obedience to the change of f_{inj} , thereby keeping the difference between the new oscillation-wave frequency f_0' and the trapped sideband-wave frequency always equal to f_{inj} . Due to the large Q-factor of the idler cavity, the sideband noise of the oscillation-wave f_0' is, then, reduced remarkably as compared to that in the free-running state.

Fig.1 illustrates the mechanism of the parametric injection locking described above. (a) shows the free-running state with a low-frequency signal f_{inj} injected. Because there is no idler cavity provided, neither noise reduction nor the oscillation-wave frequency dependence on f_{inj} occurs in this case. (b) and (c) indicate the locked state with the idler cavity trapping f_u and f_L , respectively. Here, the idler resonator is shown by a Q-curve centered at f_i . Definitions of $\Delta f_0 = f_0' - f_0$, $\Delta f_u = f_u - f_i$, and $\Delta f_L = f_L - f_i$ are also indicated in this figure.

Experiment

An experiment is carried out by using a GaAs Schottky-barrier IMPATT diode whose free-running frequency f_0 is 36.7 GHz and output power P_0 is 19.2 dBm. As the main cavity, a conventional cap-type resonator is used here, Q_{ext} of which is 50-100. An idler cavity resonator with a cylindrical TE_{011} mode and Q_{ext} of 1500-2000 is located at $\sim 4\lambda$ away from the diode. Through the bias circuit of the IMPATT oscillator, an injection signal is supplied, whose power P_{inj} is monitored at the nearest point to the diode. By using a bandpass filter, the output power P_0 of the oscillation-wave is measured separately from sideband-waves, although total power of the latter waves is always lower than P_0 by 10 dB or more.

Fig.2 shows an example of the properties in the locked state in the case of the upper-sideband trapping (Fig.1-b). Here, f_{inj} is varied with P_{inj} kept constant. f_i is selected at 1400 MHz above f_0 . When f_{inj} decreases from 1400 MHz, Δf_0 increases with a constant slope $\partial \Delta f_0 / \partial f_{inj}$ of -1, while Δf_u approaches asymptotically to a constant value, determination of which is beyond the accuracy of the measurement here. P_0 is, then, decreasing by only a little amount (not more than 1 dB over the locking bandwidth of 180 MHz).

The sideband noise of the oscillation-wave f_0' in the locked state is reduced by more than 25 dB as compared to that in the free-running state. An example is shown in Fig.3. Here, (a) is the spectrum of the oscillation-wave in the free-running state, whereas (b), (c), and (d) are spectra at the points $f_{inj} = 1390, 1360$, and 1220 MHz, respectively, in the locked state whose properties are shown in Fig.2.

The dependence of Δf_0 and P_0 upon P_{inj} with f_{inj}

kept constant is shown in Fig.4 in the case of $f_{inj} = 1310$ MHz. By increasing P_{inj} , the oscillation-wave follows the route A(A')-B(B')-C(C')-D(D'). The locked state starts at the point C(C'). When P_{inj} is decreased, the locked state lasts until the point E(E') is reached, where a jump to the point F(F') occurs and then the locked state ends. The hysteresis is always observed in the transition region between the locked and the unlocked states.

In the case of the lower-sideband trapping (Fig. 1-c), almost the same locking properties as those in the previous case ($f_i \approx f_u$) are obtained, except that Δf_0 in this case ($f_i \approx f_L$) increases with a constant slope $\partial \Delta f_0 / \partial f_{inj}$ of +1 when increasing f_{inj} .

The locking bandwidth increases in proportion to P_{inj} , and its maximum obtained here is 320 MHz and 250 MHz in the cases of $f_i \approx f_u$ and $f_i \approx f_L$, respectively. These values are much larger than that of the subharmonic injection locking and comparable with that of the fundamental-wave and the sideband-wave injection locking processes.

As can be seen from Fig.2, the frequency of the oscillation-wave in the locked state is always higher than that in the free-running state; i.e., $\Delta f_0 = f'_0 - f_0 > 0$ in the case of $f_i \approx f_u$. This is also the case in the situation of $f_i \approx f_L$. These results mean that the locking range is unsymmetrical with respect to the free-running frequency f_0 , and should be compared with the essentially symmetrical locking range in the fundamental-wave and the subharmonic injection locking processes.

Interpretation

To interpret the parametric injection locking from the view point of the circuit theory, we take the following procedures. The first step is to describe the three wave system (f'_0 , f_{inj} , and f_u) mutually interacting through the nonlinear avalanche inductance of the IMPATT diode. Equivalent circuits for each of the three frequencies can be derived from the general representation given by Gupta⁴, which is based on the Read model of the IMPATT diode. In the next step, the principle in the theory of the fundamental-wave injection locking given by Kurokawa¹ is applied to this system, from which expressions of the locking properties, the stability criterion, and noise reduction factor can be obtained. Calculation is carried out by referring to the experimental condition described above.

Fig.5 shows the locking properties derived analytically. The abscissa z is the normalized injection signal frequency shift $\{f_{inj} - (f'_0 - f_0)\} / (f'_0 - f_0)$. Four quantities, x , y , $s_1 \Delta |I_{1s}|$, and F_1 at two levels of the injection signal power P_{inj} are plotted as functions of z , where $x = \Delta f_0 / (f'_0 - f_0)$ is the normalized frequency shift of the oscillation-wave, $y = \Delta f_u / (f'_0 - f_0)$ is the normalized frequency shift of the idler (upper-sideband) wave, $s_1 \Delta |I_{1s}|$ is a quantity which is proportional to the power decrease of the oscillation-wave in the locked state as compared to that in the free-running state, and F_1 is a stability function which must be negative when a locked state is stable. In all of the characteristic curves in this figure, points on the solid lines represent stable locking states, whereas points on the broken lines show

unstable states where F_1 becomes positive. As can be seen from Fig.5, a locked state can exist only on the negative side of the z axis, where x or Δf_0 linearly increases with a slope of -1 when increasing $|z|$ (or decreasing f_{inj}), while y or Δf_u , then, initially decreases and then approaches to a certain value which is not equal to zero. The positive value of $s_1 \Delta |I_{1s}|$ on the left side of the z axis means that P_0 in the locked state is always lower, although by a little amount, than that in the free-running state. The locking range, which is equal to the maximum value of x shown by the closed circles on each $x-z$ curves, is an increasing function of P_{inj} . All of these properties are qualitatively and, in part, quantitatively in good agreement with the experimental results described above.

The calculated phase noise reduction factor H , which is defined as a ratio of the phase noise of the oscillation-wave in the locked state to that in the free-running state at the normalized off-carrier frequency $\omega_m / (f'_0 - f_0)$ of 0.001, is plotted in Fig.6 as a function of x . From this figure, it can also be seen that more than 20 dB of the phase noise reduction can be realized, which is in agreement with the experimental result, too.

Application

Following applications of the parametric injection locking are considered to be important;

- (1) as a low noise oscillator whose frequency can be varied electronically.
- (2) as an up-converter with power gain of frequency or phase modulated signal.

Experimental results on an up-converter of an FM-modulated injection signal will be given at the Symposium.

Acknowledgement

The authors wish to thank Drs. M.Fujimoto, Y.Sato, and M.Watanabe of our laboratory for their encouragement, and Prof. J.Hamasaki of the University of Tokyo for many suggestions and discussions.

References

- (1) K.Kurokawa, Proc.IEEE, 61, p.1386, Oct., 1973.
- (2) C.H.Chien et al., Electron. Lett., 6, p.240, 1970.
- (3) Y.Fukatsu et al., Proc.IEEE, 57, p.342, Mar., 1969.
- (4) M.S.Gupta, Solid-State Electron., 19, p.23, 1976.

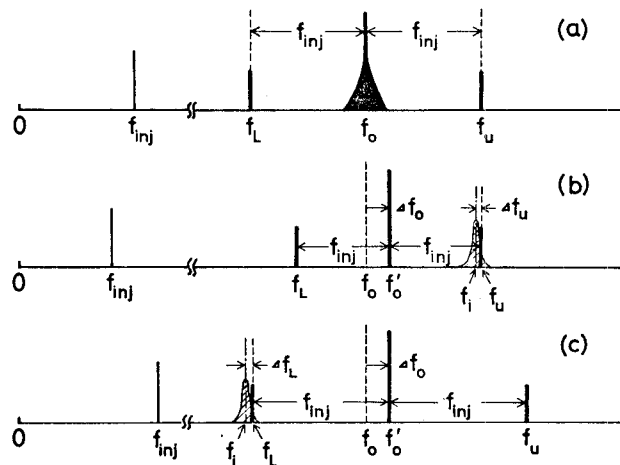


Fig.1. Spectral representation of parametric injection locking.

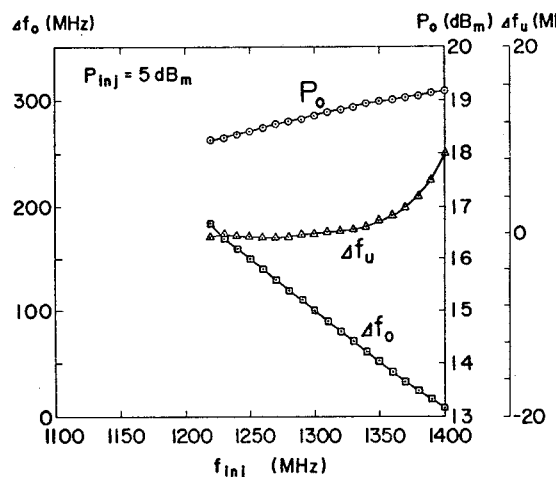


Fig.2. Characteristics within the locking-band in the $f_i \approx f_u$.

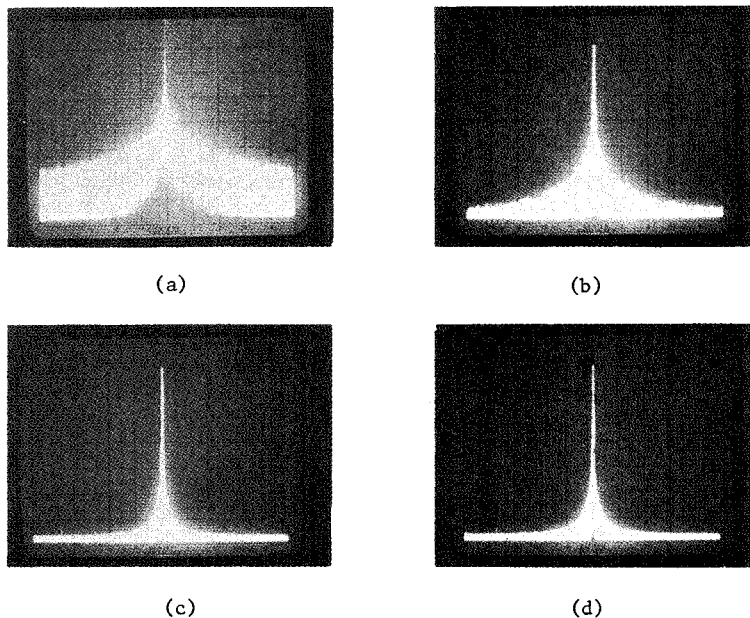
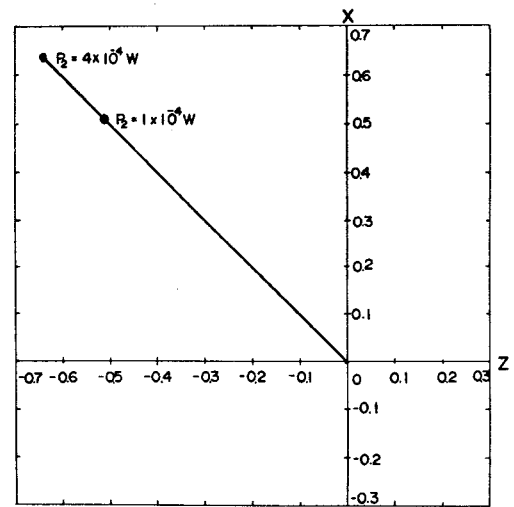


Fig.3. Photographs of spectrum of the oscillation-wave. Horizontal 1 MHz/div. Vertical 10 dB/div.

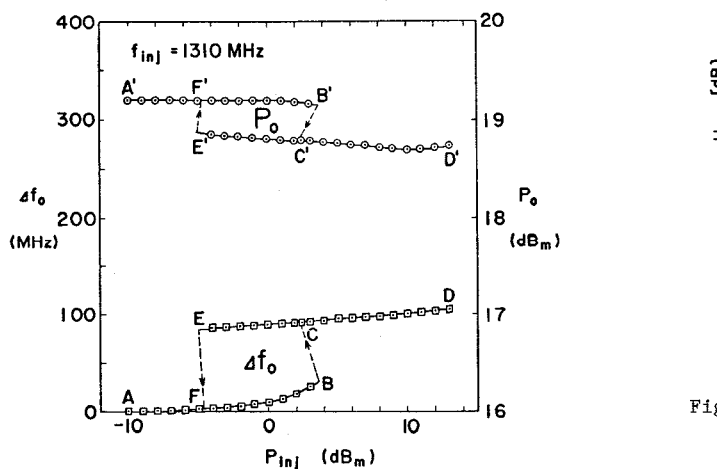


Fig.4. Transition between the locked state and the unlocked state.

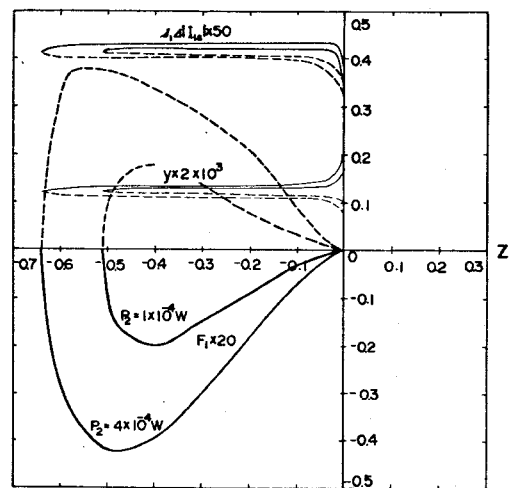


Fig.5. Locking properties derived analytically. Here, $P_2 = P_{inj}$.

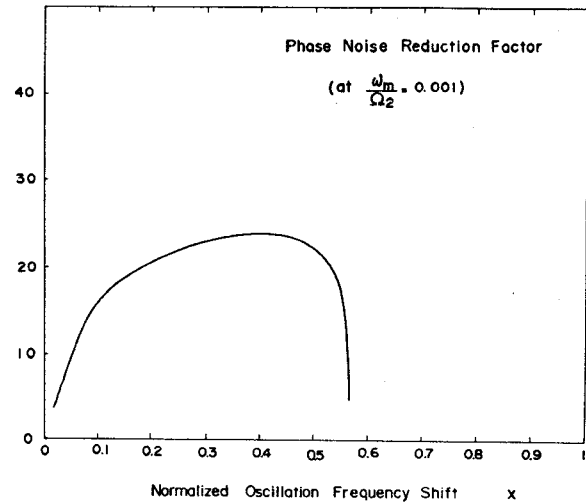


Fig.6. Analytical result on the phase noise reduction factor H v.s. the normalized oscillation frequency shift x .